Neurology®

The most widely read and highly cited peer-reviewed neurology journal
The Official Journal of the American Academy of Neurology

AMERICAN ACADEMY OF
NEUROLOGY®

Mechanisms of Network Changes in Cognitive Impairment in Multiple Sclerosis

Author(s):

Danka Jandric, MSc[1]; Ilona Lipp, PhD[2]; David Paling, MRCP, PhD[3]; David Rog, MD[4]; Gloria Castellazzi, PhD[5]; Hamied Haroon, PhD[1]; Laura Parkes, PhD[1]; Geoff Parker, PhD[1, 6]; Valentina Tomassini, MD, PhD[7, 8, 9]; Nils Muhlert, PhD[1]

Neurology® Published Ahead of Print articles have been peer reviewed and

accepted for publication. This manuscript will be published in its final form after

copyediting, page composition, and review of proofs. Errors that could affect the

content may be corrected during these processes.

Equal Author Contributions:
Danka Jandric & Ilona Lipp are co-first authors.   Valentina Tomassini & Nils Muhlert are co-senior authors.

Corresponding Author:
Nils Muhlert
nils.muhlert@manchester.ac.uk

Affiliation Information for All Authors: 1. Division of Neuroscience & Experimental Psychology, School of Biological Sciences, Faculty of Biology, Medicine and Health, University of Manchester, Manchester Academic Health Science Centre, Manchester, UK; 2. Department of Neurophysics, Max Planck Institute for Human Cognitive & Brain Sciences, Leipzig, Germany; 3. Royal Hallamshire Hospital, Sheffield Teaching Hospitals, NHS UK; 4. Salford Royal Hospital, Salford Royal NHS Foundation Trust, NHS UK; 5. NMR Research Unit, Queens Square Multiple Sclerosis Centre, University College London, London, UK, Centre for Medical Image Computing, Department of Computer Science and Department of Neuroinflammation, Queen Square Institute of Neurology, University College London, London, UK; 6. Centre for Medical Image Computing, Department of Computer Science and Department of Neuroinflammation, Queen Square Institute of Neurology, University College London, London, UK; 7. Cardiff University Brain Research Imaging Centre, Cardiff University, Cardiff, UK; 8. Institute for Advanced Biomedical Technologies (ITAB), Department of Neurosciences, Imaging and Clinical Sciences, University G. d'Annunzio of Chieti-Pescara, Chieti, Italy; 9. Multiple Sclerosis Centre, Department of Neurology, SS. Annunziata University Hospital, Chieti, Italy

Contributions:
Danka Jandric: Drafting/revision of the manuscript for content, including medical writing for content; Study concept or design; Analysis or interpretation of data
Ilona Lipp: Drafting/revision of the manuscript for content, including medical writing for content; Major role in the acquisition of data; Study concept or design; Analysis or interpretation of data
David Paling: Drafting/revision of the manuscript for content, including medical writing for content
David Rog: Drafting/revision of the manuscript for content, including medical writing for content
Gloria Castellazzi: Drafting/revision of the manuscript for content, including medical writing for content; Analysis or interpretation of data
Hamied Haroon: Drafting/revision of the manuscript for content, including medical writing for content; Analysis or interpretation of data
Laura Parkes: Drafting/revision of the manuscript for content, including medical writing for content; Study concept or design
Geoff Parker: Drafting/revision of the manuscript for content, including medical writing for content; Study concept or design; Analysis or interpretation of data
Valentina Tomassini: Drafting/revision of the manuscript for content, including medical writing for content; Major role in the acquisition of data
Nils Muhlert: Drafting/revision of the manuscript for content, including medical writing for content; Study concept or design; Analysis or interpretation of data

Number of characters in title: 75

Abstract Word count: 321

Word count of main text: 4428

References: 50

Figures: 5

Tables: 2

Disclosures: D. Jandric reports no disclosures; I. Lipp reports no disclosures;D. Paling reports personal fees from Novartis, grants and personal feels from Sanofi Genzyme, personal fees from Biogen, personal fees from Celgene, personal fees from Merck, outside the submitted work; D. Rog reports personal fees from Biogen, personal fees from MedDay, personal fees from Hikma Pharmaceuticals, grants and personal fees from Sanofi Genzyme, personal fees from Novartis, personal fees from Roche, personal fees from Janssen-Cilag, outside the submitted work;G. Castellazzi reports no disclosures; H. Haroon reports no disclosures;L. Parkes reports no disclosures; G. Parker reports grants from Medical Research Council, during the conduct of the study, grants from Engineering and Physical Sciences Research Council, outside the submitted work, and is Director of, and shareholder in, Queen Square Analytics, a company with an interest in neuroimaging services, and is Director of, and shareholder in, Bioxydyn, a company with an interest in neuroimaging services; V. Tomassini reports no disclosures;N. Muhlert reports no disclosures.

Abstract

Background and Objectives: Cognitive impairment in multiple sclerosis (MS) is associated with functional connectivity abnormalities. While there have been calls to use functional connectivity measures as biomarkers there remains to be a full understanding of why they are affected in MS. In this cross-sectional study we tested the hypothesis that functional network regions may be susceptible to disease-related 'wear-and-tear' and that this can be observable on co-occuring abnormalities on other MR metrics. We tested whether functional connectivity abnormalities in cognitively impaired MS patients co-occur with either 1) overlapping, 2) local, or 3) distal changes in anatomical connectivity and cerebral blood flow abnormalities.

Methods: Multimodal 3T MRI and assessment with the Brief Repeatable Battery of Neuropsychological tests was performed in 102 relapsing-remitting MS patients and 27 healthy controls. MS patients were classified as cognitively impaired if they scored ≥1.5 standard deviations below the control mean on ≥2 tests (n=55), or else cognitively preserved (n=47). Functional connectivity was assessed with Independent Component Analysis and dual regression of resting-state fMRI images. Cerebral blood flow maps were estimated and anatomical connectivity was assessed with anatomical connectivity mapping and fractional anisotropy of diffusion-weighted MRI. Changes in cerebral blood flow and anatomical connectivity were assessed within resting state networks that showed functional connectivity abnormalities in cognitively impaired MS patients.

Results: Functional connectivity was significantly decreased in the anterior and posterior default mode networks and significantly increased in the right and left frontoparietal

networks in cognitively impaired relative to cognitively preserved MS patients (TFCE-corrected at $p \leq 0.05$, two-sided). Networks showing functional abnormalities showed altered cerebral blood flow and anatomical connectivity locally and distally but not in overlapping locations.

Discussion: We provide the first evidence that FC abnormalities are accompanied with local cerebral blood flow and structural connectivity abnormalities but also demonstrate that these effects do not occur in exactly the same location. Our findings suggest a possibly shared pathological mechanism for altered functional connectivity in brain networks in MS.

Introduction

Cognitive impairment affects about half of people with multiple sclerosis (MS)[1]. Although the disease mechanisms responsible are not fully elucidated, resting-state functional MRI (rs-fMRI) studies have shown differences in functional connectivity (FC) between cognitively impaired and non-impaired patients[2]. However, a shortcoming of rs-fMRI, which limits the ability to interpret findings, is the lack of information about pathological mechanisms underlying FC abnormalities.

It has been proposed, in the 'nodal stress' hypothesis, that the high activity of network regions with high connectivity, so called 'hubs' or 'nodes,' makes them susceptible to pathological 'wear-and-tear,' possibly due to high metabolic demands, which could accelerate neurodegeneration, leading to network dysfunction[3,4].

If 'wear-and-tear' changes are responsible for FC abnormalities, we would expect to see abnormalities also on other MR metrics. Network hubs are heavily interconnected within both functional and structural networks, and activity-related damage can be expected to affect anatomical connectivity. In addition, if nodal damage is caused by unmet metabolic demands, this could affect cerebral blood flow (CBF)[5]. By collecting diffusion MRI and CBF data alongside rs-fMRI images we can establish whether FC abnormalities co-occur with white matter and perfusion changes, as would be expected under the 'nodal stress' hypothesis. Such co-occurring abnormalities can point to shared underlying mechanisms and thus inform the direction of future research.

In this study we tested the 'nodal stress' hypothesis in a cohort of relapsing-remitting multiple sclerosis patients (RRMS) to test whether FC abnormalities in cognitively impaired

patients co-occur with anatomical connectivity and CBF abnormalities in 1) spatially overlapping regions within networks, 2) the same networks, or 3) distal areas from resting state networks.

Methods

Participants

One hundred two patients with a diagnosis of RRMS were recruited through the Helen Durham Centre for Neuroinflammation at the University Hospital of Wales, and twenty-seven healthy controls (HC) from the community. All participants were aged between 18 and 60 years, right-handed and had no contraindications for MR scanning. Patients had no comorbid neurological or psychiatric disease, were relapse-free and had no change to treatment for 3 months prior to the MRI scan. All participants underwent MRI scanning and assessment of clinical and cognitive function in one study session.

Standard Protocol Approvals, Registrations, and Patient Consents

The study was approved by the NHS South-West Ethics and the Cardiff and Vale University Health Board R&D committees. All participants provided written informed consent to participate in the study.

Clinical and neuropsychological assessment

Clinical functioning was assessed with the Multiple Sclerosis Functional Composite (MSFC), a standardised measure of upper and lower limb and cognitive function[6].

All participants underwent neuropsychological assessment with the Brief Repeatable Battery of Neuropsychological Tests (BRB-N), a validated battery with demonstrated sensitivity to cognitive impairment in MS[7]. Patients' scores on each test were converted to Z scores based on means and standard deviations from the 27 HCs. Patients who scored ≥1.5 standard deviations below the control mean, on ≥2 tests were considered cognitively impaired (CI), a medium stringency definition of cognitive impairment[8]. Remaining patients were considered cognitively preserved (CP). Scores for each of the four cognitive domains of verbal memory, visual memory, attention, information processing and executive function, and verbal fluency, were calculated by averaging the scores for each test in that domain, as described by Sepulcre et al[8].

MRI acquisition

All participants underwent MRI examination on a 3T MR scanner (General Electric HDx MRI System, GE Medical Devices, Milwaukee, WI) using an eight channel receive-only head RF coil. A high-resolution 3D T1-weighted (3DT1) sequence was acquired for identification of T1-hypointense MS lesions, segmentation, registration and volumetric measurements [resolution 1x1x1 mm, TE = 3.0 ms, TR = 7.8 ms, matrix = 256x256x172, FOV = 256 x 256 mm, flip angle = 20°]. A T2/proton-density (PD)-weighted sequence (voxel size = 0.94x0.94x4.5 mm, TE = 9.0/80.6 ms, TR = 3000 ms, FOV = 240 x 240 mm, 36 slices) and a fluid-attenuated inversion recovery (FLAIR) sequence (voxel size = 0.86x0.86x4.5 mm, TE = 122.3 ms, TR = 9502 ms, FOV = 220 x 220 mm, 36 slices) were acquired for identification and segmentation of T2-hyperintense MS lesions. Rs-fMRI was acquired using a T2* weighted gradient-echo echo-planar (GE-EPI) imaging sequence (voxel resolution = 3.4x3.4x3 mm, TE = 35 ms, TR = 3000 ms, FOV = 220 x 220 mm, 100 volumes, 46 axial slices each in an interleaved order), During which all participants were instructed to relax with their eyes closed. Diffusion MRI (dMRI) was acquired with a twice refocused diffusion-weighted spin echo echo-planar (SE-EPI) sequence with 6 volumes with no diffusion

weighting and 40 volumes with diffusion gradients applied in uniformly distributed directions (Camino 40), b = 1200 s/mm^2, voxel size=1.8x1.8x2.4 mm, TE = 94.5 ms, TR = 16000 ms, FOV = 230 x 230 mm, 57 slices. CBF was quantified using multi-inversion time pulsed arterial spin labelling (ASL). A PICORE QUIPSS II sequence with a dual-echo gradient-echo readout and spiral k-space acquisition was employed (voxel size=3x3x8 mm, 22 slices) [9]. Sixteen tag-control pairs each for short inversion times, TI (400, 500, 600, 700 ms) and 8 tag-control pairs for long TI (1100, 1400, 1700 and 2000 ms) were acquired with QUIPSS II cut-off at 700 ms. A calibration (M_0) image was acquired to obtain the equilibrium magnetization of cerebrospinal fluid, needed for the quantification of CBF. A minimal contrast image was acquired with TE=11ms, TR=2000 ms to correct for coil inhomogeneities.

3DT1 image analysis

Structural 3DT1 images from patients were lesion filled, as described by Lipp *et al.*, 2019, to allow better segmentation of brain tissue[10], then segmented into grey matter (GM), white matter (WM) and cerebrospinal fluid (CSF) using FSL's Automated Segmentation Tool (FAST)[11]. The quality of segmentation was manually assessed. Binary masks of intracranial brain tissue excluding CSF was created from the GM and WM images, for use in dMRI analyses. Brain volumes, including whole brain volume, GM volume and WM volume were quantified from lesion-filled 3DT1 images with FSL's SIENAX tool[12]. Lesion volume was calculated from binary lesion masks created as part of lesion filling.

Rs-fMRI analysis

Rs-fMRI BOLD time-series were corrected for physiological noise in MATLAB[13] using a previously established pipeline[14]. Rs-fMRI images were pre-processed with FSL's MELODIC pipeline[15], which included motion correction, spatial smoothing with a 3 mm full width at half-maximum Gaussian kernel, high-pass temporal filtering equivalent to 0.01 Hz , non-linear registration to Montreal Neurological Institute (MNI) standard space, and

resampling to a resolution of 4 mm isotropic. Head motion parameter estimates of absolute and relative displacement values did not differ between any groups (HC-RRMS p=0.58 (absolute), p=0.27 (relative); CP-CI p=0.11 (absolute), p=0.52 (relative)).

Independent Component Analysis (ICA), part of the MELODIC pipeline, decomposed the concatenated dataset into 82 components. Four resting state networks (RSNs) which have been found to be important for cognitive function in MS were manually identified and selected for further analyses: the default mode network (DMN)[16,17], left and right frontoparietal networks (LFPN, RFPN)[16–18] and the salience network (SN)[17,19]. The anterior and posterior parts of the DMN (DMNa and DMNp, respectively)[20], were identified in two additional components. The primary visual network was used as a non-cognitive control network. Dual regression[15] was used to generate subject-specific versions of the group-average components.

dMRI analysis

Preprocessing of dMRI data was carried out in ExploreDTI (v 4.8.3[21]) and included motion correction and corrections for eddy current and EPI☐induced geometrical distortions by registering each diffusion image to its respective (skull-stripped and downsampled to 1.5 mm) 3DT1 image[22] using Elastix[23], with appropriate reorientation of the diffusion☐encoding vectors [24]. FSL's FDT tool was used to fit diffusion tensors, generate fractional anisotropy (FA) maps and fit the probabilistic diffusion model.[25,26] Processed diffusion data was quality checked manually. Anatomical connectivity maps (ACMs) were generated using FSL's Probtrackx2 tool[25,26] by seeding tractography with 50 initiated streamlines per voxel in the binary parenchymal mask. The resulting ACM maps show anatomical connectivity across the whole brain, where the magnitude of the ACM value in each voxel represents the number of probabilistic streamlines passing through that voxel[27], thus assessing the degree of anatomical interconnection of every voxel in the brain[28,29]. Each participant's ACM image was divided

by the number of voxels in the brain parenchymal mask to normalise for intracranial volume. To normalise to MNI space, the downsampled 3DT1 image of each participant was non-linearly registered to MNI space, and the warps were applied to the ACM images.

ASL analysis

The two sets of ASL tag-control images were motion corrected to the M0 image using FSL's McFLIRT tool[30], control-tag subtracted, averaged across pairs, and combined into a single multi-TI series that was fed to *oxford_asl* (BASIL)[31] for CBF quantification. CBF was estimated with partial volume correction[32], coil sensitivity correction (bias field calculated using the SPM12[33] segmentation on the minimum contrast image) and calibration with the M0 signal from subject-specific ventricle masks. CBF maps were then registered to the T1 structural scan following 6 DOF affine registration of the M_0 scan. T1-weighted images were non-linearly normalised to the Montreal Neurological Institute (MNI) 152 template space, using ANTs SyN[34] and the obtained warp was applied to the CBF maps. Full CBF maps could not be obtained for all participants due to technical problems with the MR acquisition or due to failed qualitative quality checks of the data. CBF analyses were therefore conducted on data from 49 CI and 43 CP patients. The excluded patients did not differ substantially on demographic and clinical variables from the remaining CI and CP groups.

Statistical analyses

Statistical analyses of the demographic, clinical, global MRI and median ACM, FA and CBF values were performed in SPSS version 23.0[35]. The distributions of all variables were checked with Kolmogorov-Smirnov tests and visual inspection of histograms and Q-Q plots. Variables showing a skew were analysed with non-parametric tests. To test the hypothesis that RSNs that show FC abnormalities also show ACM, FA and CBF abnormalities, we considered that ACM, FA and CBF changes could either be in the same voxel clusters that showed FC abnormalities, or elsewhere in the affected network. This was tested in analysis

steps 1 and 2. In addition, we conducted an exploratory analysis of ACM, FA and CBF changes throughout the brain to understand how widespread these are in CI compared to CP patients. The data was analysed as follows:

1. Assessment of spatially overlapping changes

Binary masks of the RSN voxels clusters that showed significant FC differences between CI and CP groups were created and used to extract local median ACM, FA and CBF values of these regions, which were then compared between CI and CP groups.

2. Assessment of local changes within RSNs

Second, we determined whether there were more diffuse changes in anatomical connectivity and CBF throughout each RSN. A binary mask of each RSN was created, and, for dMRI analyses, dilated by one voxel to include the white matter surrounding RSN regions. Voxelwise analyses of ACM, FA and CBF maps were conducted to look for abnormalities within the RSN regions. For FA, this was done both with skeletonised FA maps in a tract-based spatial statistics (TBSS) analysis[36], and with non-skeletonised FA maps. TBSS overcomes the difficulties of achieving accurate registration of the white matter by projecting all subjects' FA data onto a mean FA tract skeleton, before applying voxelwise cross-subject statistics. However, the FA skeleton includes only the centre of white matter tracts[37] and may not capture white matter local to grey matter network regions, hence we conducted both in an exploratory analysis to determine which is most sensitive to FA changes in and around RSNs. Next, we extracted median ACM, FA and CBF values from the RSNs and compared between CI and CP patients. The voxelwise analysis approach can show the spatial location of any abnormalities in the metrics studied, but requires the abnormalities to be in the same spatial location in most subjects in a group for a group difference to be detected. If this is not the case a group difference could be missed, hence we also extracted median values from our

regions of interest in an exploratory analysis. Medians, rather than means, were extracted because ACM, FA and CBF values were not normally distributed in RSN regions.

3. Diffuse changes in anatomical connectivity and CBF throughout the brain

Last, we checked whether CI and CP groups showed differences in ACM, FA and CBF throughout the brain, by running voxelwise analysis on the ACM, FA and CBF maps of the whole brain. This was an exploratory analysis to understand the spatial extent of ACM, FA and CBF abnormalities.

Comparisons, thresholding and multiple comparison correction

Comparisons of FC were conducted for both the whole RRMS group with HC, and the CI and CP patient groups to each other, to determine whether FC abnormalities are present in our RRMS cohort, and to assess how they differ between the two patient subgroups. Subsequent analyses of anatomical connectivity and cerebral blood flow were conducted only for the two patient groups to limit the number of statistical comparisons and in line with our hypotheses.

Comparisons of median ACM, FA values and CBF values were performed using a two-sample t-test or Mann-Whitney U-test, as appropriate. A Bonferroni correction for multiple comparisons, of a factor of four for the four RSNs of interest, was applied to the results. The corrected threshold was $p \leq 0.0125$.

For all voxelwise analyses, age, sex and education level were included in general linear models as covariates, and all results were threshold-free cluster enhancement (TFCE)-corrected at $p \leq 0.05$, two-sided. For rs-fMRI analyses, we calculated the percentage of network voxels showing abnormal FC between groups, and retained only those RSNs showing the largest proportion of abnormal network voxels for further analyses, in order to reduce the influence of noise. The Harvard-Oxford cortical structural, Harvard-Oxford

subcortical structural and JHU white-matter tractography atlases in FSL were used to report anatomical locations.

Data availability

Anonymised data will be shared at the request of other investigators for purposes of replicating procedures and results.

Results

Demographic, clinical, neuropsychological characteristics and conventional MRI data

Demographic and clinical characteristics of HC, RRMS patients and the CI and CP subgroups are presented in Table 1. RRMS patients and controls showed no significant differences in sex, but the RRMS group was significantly older and less educated than controls and performed worse on all MSFC tests. Fifty-five patients met the definition for CI, and 47 were considered CP. Compared to CP patients, CI patients did not differ significantly in age, sex, education, disease duration, or lower limb function, as measured by the 25 Foot Walk Test of the MSFC. However, their performance on the 9-Hole Peg Test demonstrated worse upper limb function. CI patients showed impaired cognitive function compared to CP patients and HC on all four cognitive domains assessed by the BRB-N (Table 2). The greatest impairments were observed on the information processing, attention and executive function and verbal memory domains. CP patients did not perform significantly worse than controls on any domain. RRMS patients had significantly lower normalised brain volume (NBV) and normalised GM volume (NGMV) than healthy controls, but showed no significant difference in normalised WM volume (NWMV). CI and CP groups showed no significant differences in any volumetric brain measures (Table 2).

Functional connectivity

RRMS patients showed FC abnormalities in in all RSNs investigated compared to HC.

CI patients had areas of decreased FC in the DMNa, DMN, DMNp, LFPN and primary visual network, and increased FC in areas of the DMN, SN, RFPN, LFPN and primary visual network relative to CP patients. The DMNa, DMNp, LFPN and RFPN showed the largest proportion of abnormal voxels between groups and were therefore retained for subsequent analyses (Fig 1).

Anatomical connectivity and cerebral blood flow

1. Local changes in ACM, FA and CBF in regions showing FC changes

In RSN regions that showed FC changes in CI patients compared to CP patients, there were no significant differences in median ACM, FA and CBF values between the CI and CP groups, following application of a Bonferroni correction for multiple comparisons (corrected p threshold = 0.0125).

2. Diffuse changes in connectivity within RSNs

Voxelwise analyses of ACM, FA and CBF demonstrated abnormalities in all four RSNs in CI compared to CP patients. ACM was reduced in: DMNa regions that correspond to the forceps minor, left cingulum, left anterior thalamic radiation and right anterior corona radiata; DMNp regions including parts of the splenium of the corpus callosum, left and right cingulum, forceps major and also forceps minor; RFPN white matter corresponding to parts of the right inferior longitudinal fasciculus (ILF) and the right inferior fronto-occipital fasciculus (IFOF); and LFPN regions corresponding to parts of the left superior longitudinal fasciculus, left ILF and left side of forceps major. There were also areas of increased ACM values, including

some voxels in the left superior parietal lobe and left occipital lobe in the DMNa, in a part of the left superior longitudinal fasciculus in the DMNp, the right posterior temporal lobe in the RFPN and in regions of the occipital lobe which could be in either the right ILF or right IFOF in the LFPN (Fig 2).

The TBSS analysis showed FA reductions in: the genu of the corpus callosum, forceps minor and cingulum bilaterally in the DMNa; in the splenium of the corpus callosum, posterior parts of the cingulum bilaterally and posterior corona radiata bilaterally in the DMNp; in parts of the right frontal lobe and right parietal lobe in the RFPN; and in the left side of the splenium of the corpus callosum, left side of forceps major and left cingulum in the LFPN (Fig 3A). There were also small areas of FA increases, across the frontal and parietal lobes (Fig 3B). The voxelwise analysis of non-skeletonised FA maps found FA changes in largely the same regions as the TBSS analysis (Fig 3C to D).

There were regions of reduced CBF in all four networks in CI, compared to CP patients (Fig 4). Reductions were seen in the bilateral cingulate gyrus and precuneus in the DMNa; bilateral precuneus, left cuneal cortex, right lateral occipital cortex, left lingual gyrus and left posterior cingulate gyrus in the DMNp; the right occipital cortex, right angular gyrus, right superior supramarginal gyrus and right cingulate gyrus in the RFPN. The same regions but in the left hemisphere showed CBF reductions in the LFPN. We found some individual voxels, likely artefacts, showing increased CBF in CI patients, in the DMNa, DMNp and RFPN (Fig 4).

Comparisons of extracted median values only found reduced ACM in CI patients (*Mdn* = 0.0039) compared to CP patients (*Mdn* = 00043) in the anterior DMN (*U*=897.00, *p*=0.008*),* but no other RSNs. There were no differences in median FA or CBF values in RSN regions.

3. Diffuse changes in connectivity and CBF throughout the brain – rationale and results

CI, compared to CP, had widespread ACM and FC reductions throughout the brain and some small areas of increased ACM and FC at the edges of the brain. CBF was decreased throughout the brain (Fig 5).

Discussion

In this study we provide the first evidence that abnormal FC co-occurs with altered structural connectivity and cerebral blood flow in cognitively impaired MS patients in resting state network regions. At the same time our findings reveal that the exact location of abnormalities differed between metrics. Overall, this indicates that RSNs may be vulnerable to clinically-relevant MS pathology, offering partial support for activity-related 'wear-and-tear' damage of network hubs predicted by the 'nodal stress' hypothesis[3,4].

We found FC abnormalities in our RRMS cohort relative to HC in all RSNs investigated, confirming FC changes as a widespread pathological feature in MS, as per previous studies[38]. In CI compared to CP patients, we found FC abnormalities in all networks investigated, with FC decreases in the DMNa and DMNp and increases in the RFPN and LFPN making up the highest proportion of affected network voxels. Increased FC could reflect compensatory mechanisms following structural damage, and decreased FC could be evidence of network breakdown[39,40]. However, we did not assess the extent of structural damage and can therefore only speculate about the mechanisms of directional FC change, which is an urgent research priority in this field. Nevertheless, our results are consistent with numerous previous reports of abnormal FC in these networks in patients with cognitive symptoms[16–18]. Importantly, the FC measure distinguished the two patient groups in the absence of significant differences in

conventional MR metrics, demonstrating its potential heightened sensitivity to clinically-relevant pathology in MS and highlighting the importance of understanding the mechanisms of FC changes.

As predicted, we found reduced anatomical connectivity of networks showing FC abnormalities in CI patients, with both the ACM and FA metrics. ACM is an anatomical network measure that shows whether the structural connectivity of a region is affected as a result of WM damage, regardless of where in the brain the WM damage is. It is informative of the degree of connectivity of our regions of interests, but not about the WM in and around RSN regions. To understand local tissue characteristics of RSN regions we also tested the FA metric, a measure of the directionality of diffusion within tissue, which is assumed to be largely determined by the presence of aligned axons in WM bundles[41], and can give information about local microstructural integrity in a WM tract. The specific voxels showing FC abnormalities were not those which showed structural changes in CI patients. Instead, other parts of the RSNs were affected. This, combined with widespread ACM and FA changes suggests that more diffuse, as opposed to focal, anatomical changes within RSNs are associated with cognitive impairment, and is in line with previous evidence which shows that FC changes are preceded by a high degree of structural damage[39,40].

As well as reductions, we found small regions of increased ACM and FA in all four RSNs. One possibility is that these are statistical artefacts. ACM increases could reflect an unmasking effect, whereby tracking becomes easier in regions where fibres are lost. However, Bozzali *et al.* (2011) found ACM increases in Alzheimer's patients and considered that they may be due to plasticity driven by medication. The mechanism of FA increases is not well understood, but it has been suggested that increased FA reflects changes in axonal structures such as reduced branching, decreased axon diameter, reduced packing density, or increases in myelination[41,42]. In MS, FA increases may be related to inflammatory

processes[43]. We cannot conclude which mechanisms are responsible for the ACM and FA increases in our CI group, but acknowledge the findings as important areas for future research.

Finally, we investigated CBF, which may be a response to decreased energy demand in MS[5,44]. As with ACM and FA, CBF was reduced in and around RSN regions in CI relative to CP patients, but not within the specific voxel clusters showing FC abnormalities, again pointing to diffuse rather than focal tissue abnormalities in RSNs. CBF reductions may reflect a response to decreased energy demand in the RSNs investigated, demonstrating altered metabolic function of RSN regions. However, there are suggestions that CBF changes could be due to a primary vascular insult[5], and future studies with more direct measures of metabolism, such as fluorodeoxyglucose (FDG) positron emission tomography (PET), could help elucidate the metabolic status of functional networks.

Overall, our findings show that diffuse ACM, FA and CBF abnormalities co-occur with RSN FC changes in CI MS patients, consistent with the 'nodal stress' hypothesis. The mechanism of nodal 'wear-and-tear' remains to be elucidated, and may relate to unmet metabolic demands[3,4]. There is preliminary evidence that functional networks are susceptible to metabolic changes, recently from a drosophila model where network changes resulted from neuronal metabolism[45]. Similarly, metabolic changes have been reported in demyelinated axons[46,47] and if this results in axonal damage or dysfunction that could be reflected in WM metrics in and around RSN regions. Thus, our results are not inconsistent with a role of metabolic changes in RSN regions. However, our methods are indirect measures of metabolic function. Other MR modalities, such as FDG PET, support the role of shared metabolic patterns between regions on RSNs[48], and 23Na MRI can show changes in sodium concentration in tissue, which is a measure of the energy state of axons[44]. If combined with rs-fMRI, these methods may be informative about the metabolic basis of FC changes.

There are limitations to consider when interpreting these results. First, our control group was younger and more educated than our patient cohort. We controlled for this by including age, sex and education as covariates in our analyses. Importantly, the CI and CP groups did not differ significantly on these demographic variables. We also did not investigate separate cognitive domains, but looked at overall cognition. There have been suggestions that domains may be differently affected by pathology[49] and this is an important avenue for future work. Further, we conducted several exploratory analyses to understand how best to explore changes in WM metrics and CBF in and around functional network regions. Comparisons of extracted median ACM, FA and CBF values from RSN regions showed no group differences between CI and CP patients, pointing to heterogeneity in the metrics across the regions. We conclude that the voxelwise analysis is more sensitive to group differences. The TBSS analysis and the voxelwise analysis of non-skeletonised FA maps showed FA reductions in largely the same regions. The latter additionally showed FA changes at the white-grey matter boundaries, which could reflect FA abnormalities in the grey matter, as has been reported in MS in several studies (reviewed in Inglese and Bester, 2010). However, findings of group differences at the edge of the brain and at the midline points to partial volume effects due to registration problems with non-skeletonised FA images and suggests that results need to be interpreted with caution. Related to this, we assessed metrics which are susceptible to partial volume effects. However, the same MR sequences were used for all participants, so any tissue contamination is unlikely to introduce bias in our group comparisons. Finally, we assessed whether FC, ACM, FA and CBF changes co-occur, but did not test whether these changes are correlated, which should be investigated in future studies with larger samples.

In conclusion, our study provides evidence that functional connectivity changes in cognitively impaired RRMS patients co-occur with abnormal blood flow and anatomical connectivity. This highlights the possibility of a common underlying pathological change in

resting state networks, such as altered metabolic state in cognitively impaired patients. The metabolic state of functional networks affected by MS should be further investigated with more direct methods of metabolic brain function to determine the pathological basis of functional connectivity abnormalities and potentially lead to their use as effective biomarkers of disease.

References

1.   Sumowski JF, Benedict R, Enzinger C, et al. Cognition in multiple sclerosis: State of the field and priorities for the future. Neurology. 2018;90:278–288.

2.   Benedict RHB. Cognition in multiple sclerosis: Charcot was right. Lancet Neurol. Elsevier Ltd; 2020;19:810.

3.   Buckner RL, Sepulcre J, Talukdar T, et al. Cortical hubs revealed by intrinsic functional connectivity: Mapping, assessment of stability, and relation to Alzheimer's disease. J Neurosci. 2009;29:1860–1873.

4.   Zhou J, Gennatas ED, Kramer JH, Miller BL, Seeley WW. Predicting Regional Neurodegeneration from the Healthy Brain Functional Connectome. Neuron. 2012;73:1216–1227.

5.   Lapointe E, Li DKB, Traboulsee AL, Rauscher A. What Have We Learned from Perfusion MRI in Multiple Sclerosis? AJNR Am J Neuroradiol. 2018;39:994–1000.

6.   Cutter GR, Baier ML, Rudick RA, et al. Development of a multiple sclerosis functional composite as a clinical trial outcome measure. Brain. 1999;122:871–882.

7.   Amato M, Portaccio E, Goretti B, et al. The Rao's Brief Repeatable Battery version B: Normative values with age, education and gender corrections in an Italian population. Mult Scler. 2006;12:787–793.

8.   Sepulcre J, Vanotti S, Hernández R, et al. Cognitive impairment in patients with

multiple sclerosis using the Brief Repeatable Battery-Neuropsychology test. Mult

Scler. 2006;12:187–195.

9. Warnert EAH, Murphy K, Hall JE, Wise RG. Noninvasive assessment of arterial

compliance of human cerebral arteries with short inversion time arterial spin labeling.

J Cereb Blood Flow Metab. Nature Publishing Group; 2015;35:461–468.

10. Lipp I, Jones DK, Bells S, et al. Comparing MRI metrics to quantify white matter

microstructural damage in multiple sclerosis. Hum Brain Mapp. 2019;40:2917–2932.

11. Zhang Y, Brady M, Smith S. Segmentation of brain MR images through a hidden

Markov random field model and the expectation-maximization algorithm. IEEE Trans

Med Imaging. 2001;20:45–57.

12. Smith SM, Zhang Y, Jenkinson M, et al. Accurate, robust, and automated longitudinal

and cross-sectional brain change analysis. Neuroimage. Elsevier; 2002;17:479–489.

13. The MathWorks I. Matlab and Statistics Toolbox Release R2011a. Natick,

Massaschusetts, United States;

14. Lipp I, Murphy K, Wise RG, Caseras X. Understanding the contribution of neural and

physiological signal variation to the low repeatability of emotion-induced BOLD

responses. Neuroimage. The Authors; 2014;86:335–342.

15. Beckmann CF, Mackay CE, Filippini N, Smith SM. Group comparison of resting-state

FMRI data using multi-subject ICA and dual regression. OHBM. 2009.

16. Meijer KA, Eijlers AJCC, Douw L, et al. Increased connectivity of hub networks and

cognitive impairment in multiple sclerosis. Neurology. 2017;88:2107–2114.

17. Cruz-Gómez ÁJ, Ventura-Campos N, Belenguer A, Ávila C, Forn C. The link between

resting-state functional connectivity and cognition in MS patients. Mult Scler J.

2014;20:338–348.

18. Louapre CC, Perlbarg V, Garcia-Lorenzo D, et al. Brain networks disconnection in

early multiple sclerosis cognitive deficits: An anatomofunctional study. Hum Brain

Mapp. 2014;35:4706–4717.

19. Rocca MA, Valsasina P, Martinelli V, et al. Large-scale neuronal network dysfunction in relapsing-remitting multiple sclerosis. Neurology. 2012;79:1449–1457.

20. Xu X, Yuan H, Lei X. Activation and Connectivity within the Default Mode Network Contribute Independently to Future-Oriented Thought. Sci Rep. Nature Publishing Group; 2016;6:21001.

21. Leemans A, Jeurissen B, Sijbers J, Jones DK. ExploreDTI: a graphical toolbox for processing, analyzing, and visualizing diffusion MR data. Proc Intl Soc Mag Reson. 2009;17:3537.

22. Irfanoglu MO, Walker L, Sarlls J, Marenco S, Pierpaoli C. Effects of image distortions originating from susceptibility variations and concomitant fields on diffusion MRI tractography results. Neuroimage. 2012;61:275–288.

23. Klein S, Staring M, Murphy K, Viergever MA, Pluim JPW. elastix: a toolbox for intensity-based medical image registration. IEEE Trans Med Imaging. 2010;29:196–205.

24. Leemans A, Jones DK. The B-matrix must be rotated when correcting for subject motion in DTI data. Magn Reson Med. 2009;61:1336–1349.

25. Behrens TEJ, Woolrich MW, Jenkinson M, et al. Characterization and Propagation of Uncertainty in Diffusion-Weighted MR Imaging. Magn Reson Med. 2003;50:1077–1088.

26. Behrens TEJ, Berg HJ, Jbabdi S, Rushworth MFS, Woolrich MW. Probabilistic diffusion tractography with multiple fibre orientations: What can we gain? Neuroimage. 2007;34:144–155.

27. Bozzali M, Parker GJM, Serra L, et al. Anatomical connectivity mapping: A new tool to assess brain disconnection in Alzheimer's disease. Neuroimage. 2011;54:2045–2051.

28. Embleton K, Morris DM, Haroon HA, Lambon Ralph MA, Parker GJ. Anatomical Connectivity Mapping. Proc Int Soc Magn Reson Med. 2007;15:1548.

29. Cercignani M, Embleton K, Parker GJM, Bozzali M. Group-averaged anatomical connectivity mapping for improved human white matter pathway visualisation. NMR Biomed. 2012;25:1224–1233.

30. Jenkinson M, Bannister P, Brady M, Smith S. Improved Optimization for the Robust and Accurate Linear Registration and Motion Correction of Brain Images. Neuroimage. 2002;17:825–841.

31. Chappell MA, Groves AR, Whitcher B, Woolrich MW. Variational Bayesian Inference for a Nonlinear Forward Model. IEEE Trans Signal Process. 2009;57:223–236.

32. Chappell MA, Groves AR, MacIntosh BJ, Donahue MJ, Jezzard P, Woolrich MW. Partial volume correction of multiple inversion time arterial spin labeling MRI data. Magn Reson Med. United States; 2011;65:1173–1183.

33. Debernard L, Melzer TR, Van Stockum S, et al. Reduced grey matter perfusion without volume loss in early relapsing-remitting multiple sclerosis. J Neurol Neurosurg Psychiatry. 2014;85:544–551.

34. Avants BB, Epstein CL, Grossman M, Gee JC. Symmetric Diffeomorphic Image Registration with Cross-Correlation: Evaluating Automated Labeling of Elderly and Neurodegenerative Brain. Med Image Anal. 2008;12:26–41.

35. IMB Corp. IMB SPSS Statistics for Macintosh, Version 23.0. Armonk, NY, NY: IBM Corp; 2015.

36. Smith SM, Jenkinson M, Johansen-Berg H, et al. Tract-based spatial statistics: voxelwise analysis of multi-subject diffusion data. Neuroimage. United States; 2006;31:1487–1505.

37. Smith SM, Kindlmann G, Jbabdi S. Tract-Based Spatial Statistics and Other Approaches for Cross-Subject Comparison of Local Diffusion MRI Parameters. Brain Mapp. An Encycl. Ref. Elsevier Inc.; 2015.

38. Filippi M, Agosta F, Spinelli EG, et al. Imaging resting state brain function in multiple sclerosis. J Neurol. 2013;260:1709–1713.

39. Schoonheim MM, Meijer KA, Geurts JJGG. Network collapse and cognitive impairment in multiple sclerosis. Front Neurol. 2015;6:82.

40. Tewarie P, Steenwijk MD, Brookes MJ, et al. Explaining the heterogeneity of functional connectivity findings in multiple sclerosis: An empirically informed modeling study. Hum Brain Mapp. United States; 2018;39:2541–2548.

41. Beaulieu C. The basis of anisotropic water diffusion in the nervous system - A technical review. NMR Biomed. 2002;15:435–455.

42. Hoeft F, Barnea-Goraly N, Haas BW, et al. More is not always better: Increased fractional anisotropy of superior longitudinal fasciculus associated with poor visuospatial abilities in Williams syndrome. J Neurosci. 2007;27:11960–11965.

43. Calabrese M, Rinaldi F, Seppi D, et al. Cortical diffusion-tensor imaging abnormalities in multiple sclerosis: A 3-year longitudinal study. Radiology. 2011;261:891–898.

44. Paling D, Golay X, Wheeler-Kingshott C, Kapoor R, Miller D. Energy failure in multiple sclerosis and its investigation using MR techniques. J Neurol. 2011;258:2113–2127.

45. Mann K, Deny S, Ganguli S, Clandinin T. Causal coupling between neural activity, metabolism, and behavior across the Drosophila brain. Nature. Springer US; Epub 2020.

46. Craner MJ, Newcombe J, Black JA, Hartle C, Cuzner ML, Waxman SG. Molecular changes in neurons in multiple sclerosis: Altered axonal expression of Nav1.2 and Nav1.6 sodium channels and Na+/Ca2+ exchanger. Proc Natl Acad Sci. 2004;101:8168–8173.

47. Foster RE, Whalen CC, Waxman SG. Reorganization of the axon membrane in demyelinated peripheral nerve fibers: morphological evidence. Science. 1980;210:661–663.

48. Savio A, Fünger S, Tahmasian M, et al. Resting-state networks as simultaneously measured with functional MRI and PET. J Nucl Med. 2017;58:1314–1317.

49.	Migliore S, Ghazaryan A, Simonelli I, et al. Validity of the minimal assessment of cognitive function in multiple sclerosis (MACFIMS) in the Italian population. Neurol Sci. 2016;37:1261–1270.

50.	Inglese M, Bester M. Diffusion imaging in multiple sclerosis: research and clinical implications. NMR Biomed. 2010;23:865–872.
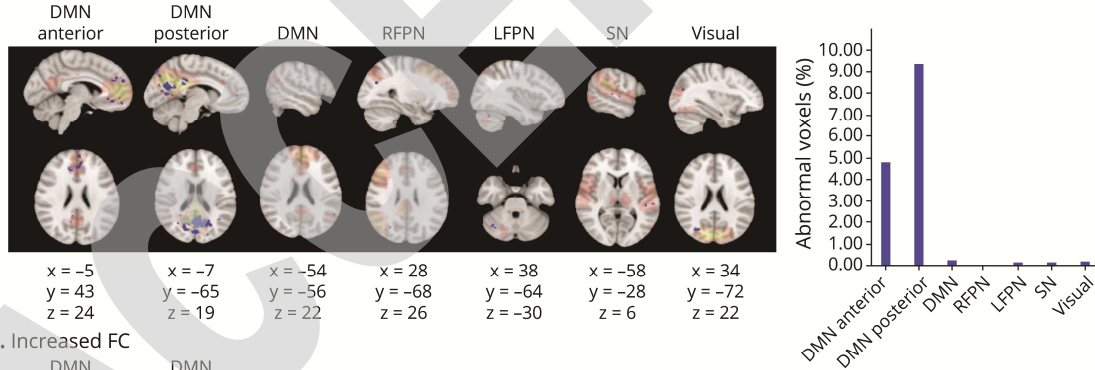
Figure 1. Functional connectivity abnormalities in cognitively impaired compared to cognitively preserved patients

Figure shows voxels showing FC abnormalities in CI compared to CP, overlaid onto the group average spatial map of each RSN analysed in red-yellow. First seven columns in each panel show each of the RSNs investigated: DMN anterior, DMN posterior, DMN, RFPN, LFPN, SN and primary visual network. For networks not displayed, no significant group differences were found. The eight column shows graphs indicating the percentage of voxels showing abnormalities, of the total number of voxels in the network. Rows show areas of: a) decreased FC in the CI group vs CP (in blue); b) increased FC in CI group (in green). Results were TFCE-corrected at $p \leq 0.05$, two-sided. MNI coordinates are given for results displayed. Colour bar shows signal intensity of RSNs.

A. Decreased FC

DMN anterior	DMN posterior	DMN	RFPN	LFPN	SN	Visual
x = –5	x = –7	x = –54	x = 28	x = 38	x = –58	x = 34
y = 43	y = –65	y = –56	y = –68	y = –64	y = –28	y = –72
z = 24	z = 19	z = 22	z = 26	z = –30	z = 6	z = 22

B. Increased FC

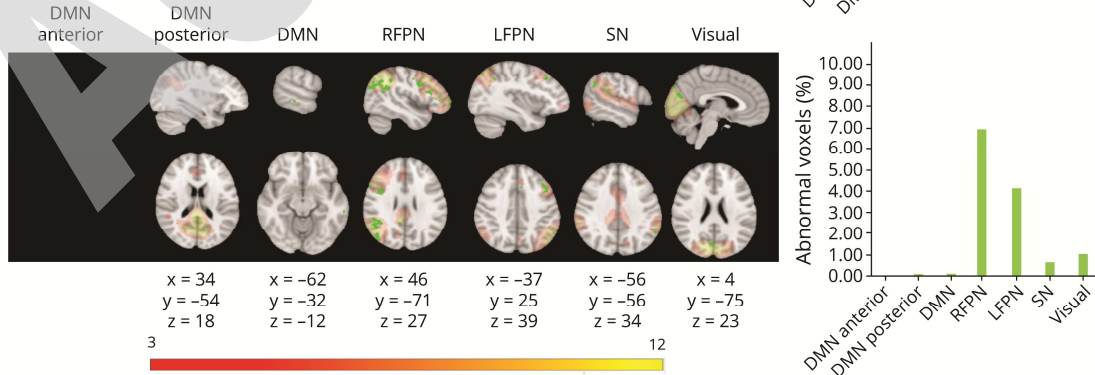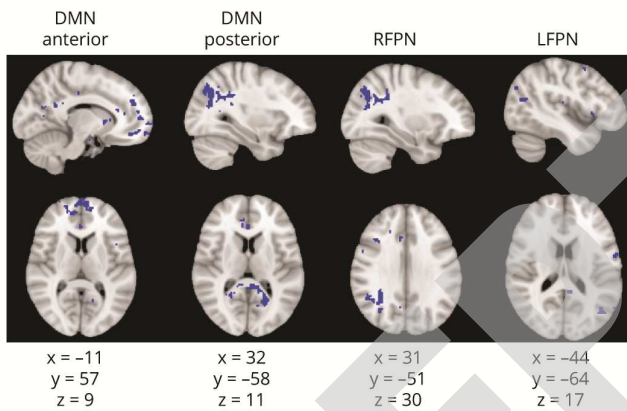| DMN anterior	DMN posterior	DMN	RFPN	LFPN	SN	Visual
	x = 34	x = –62	x = 46	x = –37	x = –56	x = 4
	y = –54	y = –32	y = –71	y = 25	y = –56	y = –75
	z = 18	z = –12	z = 27	z = 39	z = 34	z = 23

Figure 2. Anatomical connectivity changes in CI compared to CP patients, based on a voxelwise analysis of anatomical connectivity maps

Figure shows voxels showing ACM value abnormalities. Columns show each of the RSNs compared. The first row, part a), shows areas of decreased ACM values (in blue), the second row, part b), areas of increased ACM values (in red). MNI coordinates are given for the biggest voxel clusters displayed. Results were TFCE-corrected at $p \leq 0.05$, two-sided
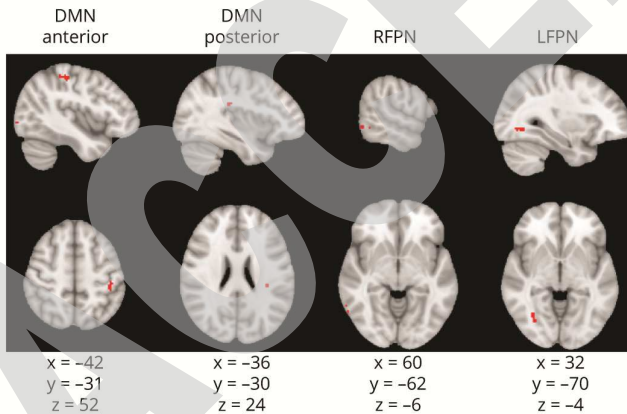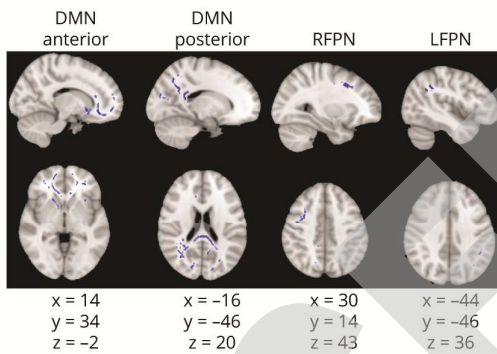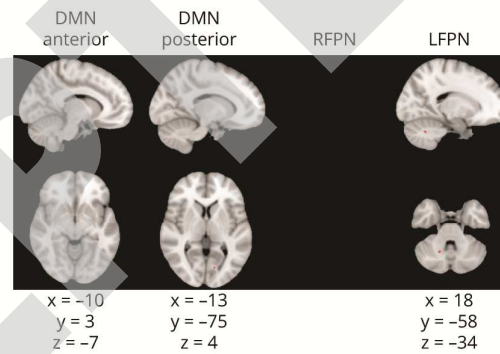

A. Decreased ACM

B. Increased ACM

Figure 3. FA changes in CI compared to CP patients

Figure shows voxels showing FA abnormalities. Parts a) and b) show results from the TBSS analysis. Parts c) and d) show results from the voxelwise analysis of non-skeletonised FA maps. Columns show each of the RSNs compared. The first row shows areas of decreased FA (in blue), the second row areas of increased FA (in red). MNI coordinates are given for the biggest voxel clusters displayed. For networks not displayed, no significant results were found. Results were TFCE-corrected at $p \leq 0.05$, two-sided.
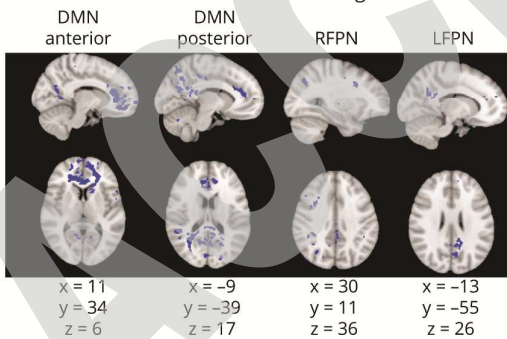

A. Decreased FA TBSS analysis

DMN anterior	DMN posterior	RFPN	LFPN
x = 14	x = −16	x = 30	x = −44
y = 34	y = −46	y = 14	y = −46
z = −2	z = 20	z = 43	z = 36

B. Increased FA TBSS analysis

DMN anterior	DMN posterior	RFPN	LFPN
x = −10	x = −13		x = 18
y = 3	y = −75		y = −58
z = −7	z = 4		z = −34

C. Decreased FA nonskeletonized images

DMN anterior	DMN posterior	RFPN	LFPN
x = 11	x = −9	x = 30	x = −13
y = 34	y = −39	y = 11	y = −55
z = 6	z = 17	z = 36	z = 26

D. Increased FA nonskeletonized images

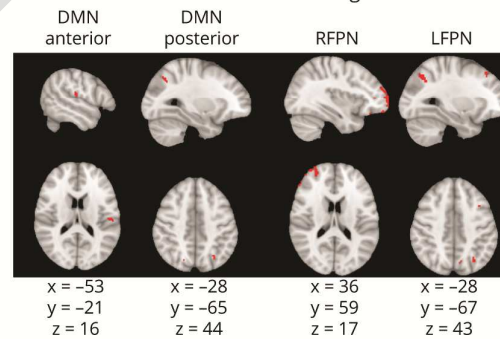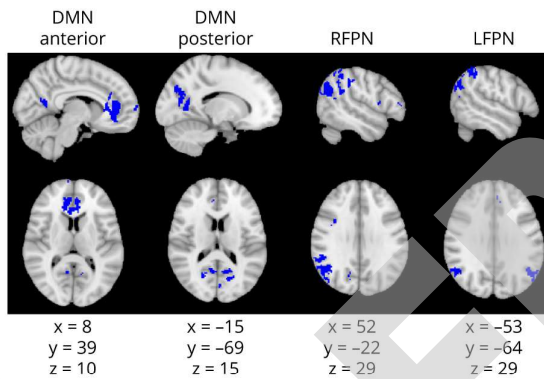| DMN anterior	DMN posterior	RFPN	LFPN
x = −53	x = −28	x = 36	x = −28
y = −21	y = −65	y = 59	y = −67
z = 16	z = 44	z = 17	z = 43

Figure 4. CBF changes in CI compared to CP patients, based on a voxelwise analysis of CBF maps

Figure shows voxels showing CBF abnormalities in red. Columns show each of the RSNs compared. The first row, part a), shows areas of decreased CBF (in blue), the second row, part b), areas of increased CBF (in red). MNI coordinates are given for the biggest voxel clusters displayed. Results were TFCE-corrected at $p \leq 0.05$, two-sided.

A. Decreased CBF

DMN anterior	DMN posterior	RFPN	LFPN
x = 8	x = −15	x = 52	x = −53
y = 39	y = −69	y = −22	y = −64
z = 10	z = 15	z = 29	z = 29

B. Increased CBF

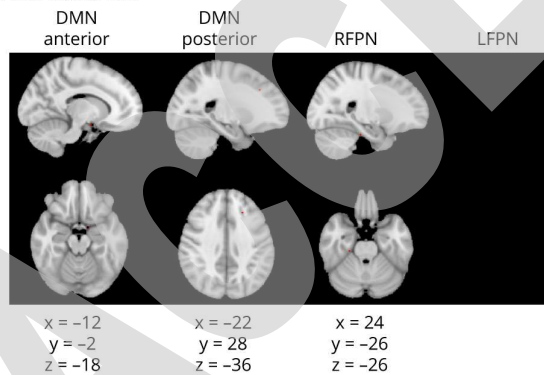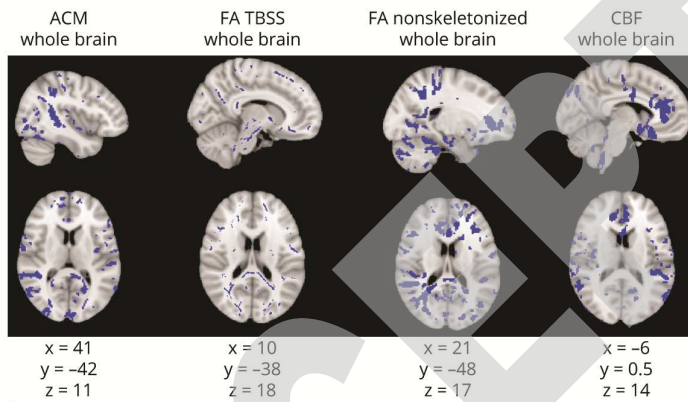| DMN anterior	DMN posterior	RFPN	LFPN
x = −12	x = −22	x = 24	
y = −2	y = 28	y = −26	
z = −18	z = −36	z = −26	

Figure 5. Diffuse ACM, FA and CBF changes across the whole brain in CI compared to CP patients

Figure shows ACM, FA and CBF abnormalities throughout the brain. Columns show each of the metrics assessed: ACM, FA from TBSS, FA from analysis of non-skeletonised FA maps, and CBF, in that order. The first row, part a), shows areas of decreased values (in blue), the second row, part b), areas of increased values (in red). MNI coordinates are given for the biggest voxel clusters displayed. Results were TFCE-corrected at $p \leq 0.05$, two-sided.

A. Decreased values

ACM whole brain	FA TBSS whole brain	FA nonskeletonized whole brain	CBF whole brain
x = 41	x = 10	x = 21	x = –6
y = –42	y = –38	y = –48	y = 0.5
z = 11	z = 18	z = 17	z = 14

B. Increased values

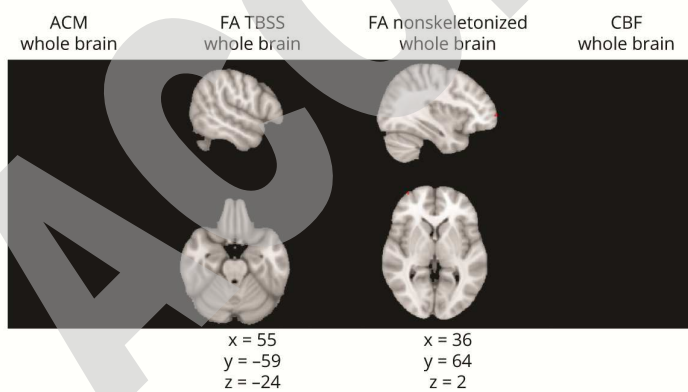| ACM whole brain	FA TBSS whole brain	FA nonskeletonized whole brain	CBF whole brain
	x = 55	x = 36	
	y = –59	y = 64	
	z = –24	z = 2	

Table 1. Demographic and clinical characteristics

	HC (n=27)	RRMS (n=102)	*Inferential test results HC-RRMS comparisons*	RRMS CP (n=47)	RRMS CI (n=55)	*Inferential test results CI-CP comparisons*
Demographic characteristics						
Age, yr (median, range)	37.00 (23-59)	45.00 (18-60)	$U = 958.00, p = .015$	42.00 (18-60)	47.00 (20-60)	$U = 1069.50, p = .134$
Male/female, n	12/15	33/69	$\chi^2(1) = 1.37, p = .241$	11/36	22/33	$\chi^2(1) = 3.19, p = .074$
Education years (median, range)	19.00 (12-30)	15.00 (10-30)	$U = 613.50, p < 0.001$	15.00 (10-27)	14.00 (10-30)	$U = 1084.50, p = .161$
Disease duration, yr (median, range)	N/A	12.24 (1-39)	N/A	11.50 (2-37)	12 (1-39)	$U = 1232.50, p = .803$
MSFC						
25 Foot Walk Test (median, range)	4.35 (3.2-5.4)	5.25 (3.6-26.8)	$U = 572.50, p < 0.001$	5.15 (3.7-13.0)	5.43 (3.6-26.8)	$U = 1169.50, p = .498$

	18.65 (15.35-23.00)	21.75 (16.35-59.50)	$U = 537.50$, $p < 0.001$	21.45 (17.15-44.85)	21.95 (16.35-59.5)	$U = 956.00$, $p = .024$
9-Hole Peg Test (median, range)						
PASAT3 (median, range)	51.00 (35-59)	43.50 (0-60)	$U = 715.00$, $p < 0.001$	50.00 (30-60)	34.00 (0-58)	$t(83.10) = 6.50$, $p < 0.001$

Independent samples t-tests were used for group comparisons of variables with a normal distribution. Those variables which were not normally distributed were assessed with Mann-Whitney U tests. Categorical variables were tested with the chi-squared test. Abbreviations: CI = cognitively impaired; CP = cognitively preserved; HC = healthy controls; MSFC = Multiple Sclerosis Functional Composite; PASAT3 = Paced Auditory Serial Addition Test; RRMS = relapsing remitting multiple sclerosis.

Table 2. Neuropsychological and MRI volumetric measures

	HC (n=27)	RRMS (n=102)	*Inferential test results* *HC-RRMS comparisons*	RRMS CP (n=47)	RRMS CI (n=55)	*Inferential test results* *CI-CP comparisons* *HC-CI-CP comparison of BRB-N*
BRB-N Z-scores						
Verbal memory (mean, SD)	0.00 (0.92)	*	N/A	0.07 (0.071)	-1.53 (1.09)	$F(2, 125) = 44.82$, $p <.001$ Post hoc: HC-CI $p < .001$, HC-CP $p = .931$, CP-CI $p < .001$
Visual Memory (mean, SD)	0.00 (0.92)	*	N/A	-0.13 (0.93)	-1.20 (1.01)	$F(2, 126) = 22.36$, $p <.001$ Post hoc: HC-CI $p < .001$, HC-CP $p = .883$, CP-CI $p < .001$
Information processing, attention, executive function (mean, SD)	0.00 (0.75)	*	N/A	-0.37 (0.73)	-1.90 (1.26)	$F(2, 126) = 44.58$, $p <.001$ Post hoc: HC-CI $p < .001$, HC-CP $p = .298$, CP-CI $p < .001$
Verbal fluency (mean, SD)	0.00 (1.00)	*	N/A	0.08 (0.72)	-0.51 (0.93)	$F(2, 125) = 6.33$, $p =.002$ Post hoc: HC-CI $p = .04$, HC-CP $p = .932$, CP-CI $p = .003$

MRI volume measures						
NBV, L (median, range)	1.55 (1.42-1.70)	1.55 (1.42-1.70)	$t(41.94) = 3.33, p = .002$	1.50 (1.37-1.66)	1.51 (1.30-1.68)	$t(99.83) = 0.36, p = .721$
NGMV, L (median, range)	0.81 (0.72-0.89)	0.77 (0.61-0.89)	$U = 755.00, p < 0.001$	0.77 (0.61-0.89)	0.76 (0.62-0.88)	$t(99.83) = 1.48, p = .142$
NWMV, L (median, range)	0.76 (0.68-0.81)	0.74 (0.66-0.83)	$t(40.43) = 1.56, p = .127$	0.74 (0.66-0.81)	0.75 (0.66-0.83)	$t(97.31) = -1.24, p = .218$
LV, mL (median, range)	N/A	*		9.73 (0.64-63.32)	9.73 (0.69-59.64)	$U = 1258.00, p = .817$

Independent samples t-tests were used for group comparisons of variables with a normal distribution. Those variables which were not normally distributed were assessed with Mann-Whitney U tests. Categorical variables were tested with the chi-squared test. BRB-N Z-scores were tested with a one-way ANOVA and Tukey's post hoc test. *RRMS group averages not calculated.

Abbreviations: BRB-N = Brief Repeatable Battery of Neuropsychological Tests; CI = cognitively impaired; CP = cognitively preserved; HC = healthy controls; LV = lesion volume; NBV = normalised brain volume; NGMV = normalised grey matter volume; NWMV = normalised white matter volume; RRMS = relapsing remitting multiple sclerosis; SD = standard deviation

Neurology®

Mechanisms of Network Changes in Cognitive Impairment in Multiple Sclerosis

Danka Jandric, Ilona Lipp, David Paling, et al.

This information is current as of October 14, 2021

Updated Information & **Services**	including high resolution figures, can be found at: http://n.neurology.org/content/early/2021/10/14/WNL.0000000000012834.full
Subspecialty Collections	This article, along with others on similar topics, appears in the following collection(s): **DWI** http://n.neurology.org/cgi/collection/dwi **fMRI** http://n.neurology.org/cgi/collection/fmri **MRI** http://n.neurology.org/cgi/collection/mri **Multiple sclerosis** http://n.neurology.org/cgi/collection/multiple_sclerosis
Permissions & Licensing	Information about reproducing this article in parts (figures,tables) or in its entirety can be found online at: http://www.neurology.org/about/about_the_journal#permissions
Reprints	Information about ordering reprints can be found online: http://n.neurology.org/subscribers/advertise

AMERICAN ACADEMY OF
NEUROLOGY®